Control of ion selectivity in potassium channels by electrostatic and dynamic properties of carbonyl ligands

Sergei Yu. Noskov[1]*, Simon Bernèche[2] & Benoît Roux[1]

[1]*Department of Biochemistry & Structural Biology, Weill Medical College of Cornell University, 1300 York Avenue, New York, New York 10021, USA*
[2]*Division of Structural Biology, Biozentrum, University of Basel Klingelbergstrasse 70, CH-4056 Basel, Switzerland*

* Permanent address: Institute of Solution Chemistry, Russian Academy of Sciences, 1, Akademicheskaya street, 153045, Ivanovo, Russia

Potassium channels are essential for maintaining a normal ionic balance across cell membranes. Central to this function is the ability of such channels to support transmembrane ion conduction at nearly diffusion-limited rates while discriminating for K^+ over Na^+ by more than a thousand-fold. This selectivity arises because the transfer of the K^+ ion into the channel pore is energetically favoured, a feature commonly attributed to a structurally precise fit between the K^+ ion and carbonyl groups lining the rigid and narrow pore[1]. But proteins are relatively flexible structures[2,3] that undergo rapid thermal atomic fluctuations larger than the small difference in ionic radius between K^+ and Na^+. Here we present molecular dynamics simulations for the potassium channel KcsA, which show that the carbonyl groups coordinating the ion in the narrow pore are indeed very dynamic ('liquid-like') and that their intrinsic electrostatic properties control ion selectivity. This finding highlights the importance of the classical concept of field strength[4]. Selectivity for K^+ is seen to emerge as a robust feature of a flexible fluctuating pore lined by carbonyl groups.

Selective conduction of K^+ is conferred by the narrowest region of the pore formed by the backbone carbonyl groups of the residue sequence TTVGYG, which is highly conserved among all known potassium channels (Fig. 1)[5–7]. Although equilibrium and non-equilibrium aspects must both be taken into consideration to address this question completely, the observed selectivity of KcsA for K^+ can largely be explained thermodynamically: partitioning of the more strongly solvated Na^+ ions into the narrow pore is unfavourable[8–10], reflected in a difference between the free energy of K^+ and Na^+ in the pore and in the bulk solution

$$\Delta\Delta G(K^+ \rightarrow Na^+) = [(G_{pore}(Na^+) - G_{bulk}(Na^+)) - (G_{pore}(K^+) - G_{bulk}(K^+))] \quad (1)$$

that is larger than zero. Ion-flux measurements[11–13] indicate that the relative free energy of selectivity $\Delta\Delta G$ is of the order of 5–6 kcal mol^{-1} for K^+ channels. This preference for K^+ ions is usually explained by pointing out that the channel can compensate for the desolvation of a cation of the correct radius like K^+ because it fits snugly into the narrow pore, whereas a sufficiently favourable interaction is not possible in the case of a smaller ion such as Na^+ (refs 1, 5, 7). This explanation is consistent with the observation that the selectivity filter in the X-ray structure of the KcsA channel is well adapted to coordinate K^+ (refs 5, 7). However, the atomic radii of K^+ and Na^+ differ only by 0.38 Å (ref. 14), so the snug-fit mechanism requires the selectivity filter to rigidly retain a precise (sub-ångstrom) geometry to discriminate between these two cations, even though proteins are 'soft materials' displaying significant structural flexibility[2,3,15]. The crystallographic thermal B-factors of the KcsA X-ray structure determined at 2.0 Å resolution are indicative of root-mean-square (r.m.s.) fluctuations of the order of about 0.75 Å (see also Supplementary Information)[7], in general accord with the structural fluctuations seen in molecular dynamics (MD) simulations of the KcsA channel[16–22]. The experimental observation that K^+ is needed for the overall stability of the channel structure[23,24] further supports the notion of a structurally flexible pore. In fact, the diameter of some regions of the pore in the X-ray structure is smaller than the size of K^+ (ref. 7), so flexibility and fluctuations seem to be essential for rapid conduction[19]. MD free-energy perturbation (FEP) computations help to elucidate the origin of energetic factors in dynamic structures[16–19], which in the case of a KcsA channel with full structural flexibility yielded ion selectivity in agreement with experimental estimates[11–13], despite atomic fluctuations of the order of ~1.0 Å r.m.s. (Fig. 1). Taken together, these observations indicate that a snug structural fit of K^+ inside the narrow and rigid pore is not the origin of the ion selectivity seen in potassium channels.

An alternative explanation is that selectivity might arise locally, from the intrinsic physical properties of the ligands coordinating the ions passing through the channel[25]. The most important local interactions are the very strong electrostatic attraction and core repulsion between the cation and the nearest carbonyl groups, and the moderate electrostatic repulsion between the coordinating carbonyl groups themselves. To probe their role in achieving ion selectivity, we monitor changes in $\Delta\Delta G$ upon artificially disrupting these interactions. The effect of turning off the electrostatic interaction between the carbonyls on $\Delta\Delta G$ is particularly informative because it is associated with the dynamical properties of the coordination shell (that is, $\Delta\Delta G$ should not be affected if the coordination structure is rigid). In the following, we compare and contrast the results from FEP computations with and without carbonyl electrostatic repulsion in the KcsA channel with those

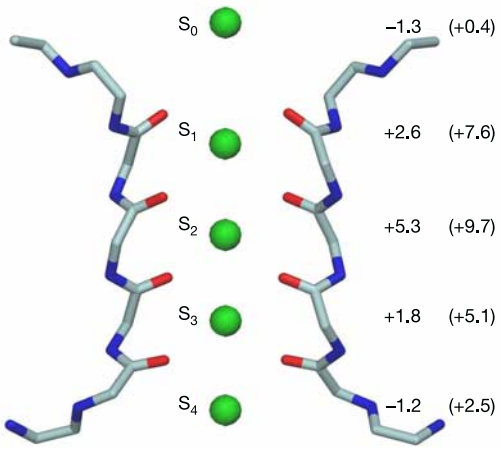

Figure 1 Schematic structure of the cation binding sites in the selectivity filter of the KcsA channel[7]. Only two subunits are depicted for clarity. The extracellular side is on the top and the intracellular side is at the bottom. Results from both X-ray crystallography[7] and MD free-energy simulations[19] show that five specific cation binding sites (S_0 to S_4) are disposed along the narrow pore of the KcsA K^+ channel. The cation positions are represented (green) and the carbonyl oxygen group of residues Thr 75, Val 76, Gly 77 and Tyr 78 are shown explicitly (red). Computational studies show that ion movement through the channel takes place in a concerted way, as the K^+ in the pore undergo hopping transitions between stable multi-ion configurations: [S_3, S_1] ↔ [S_4, S_2, S_0] ↔ [S_4, S_2] ↔ [S_3, S_1] (ref. 20), consistent with structural data[6,7]. Only configurations in which the cations are separated by one water molecule are allowed. The numbers adjacent to the binding sites are the $\Delta\Delta G$ (in kcal mol^{-1}) obtained from FEP computations based on the KcsA channel in a fully solvated lipid membrane (see Methods). Similar computations based on a frozen channel structure perfectly adapted to K^+ indicate that it is very selective (numbers in parentheses).

obtained in liquid N-methylacetamide (NMA), a generic model of the protein backbone, and valinomycin, a cationic membrane carrier exhibiting a very high selectivity for K^+ over Na^+ (refs 26, 27). The FEP calculations for the KcsA channel are focused on the site S_2, located near the middle of the narrow pore, which is the most selective (Fig. 1). The results are reported in Table 1.

Removing the carbonyl–carbonyl interaction in a fully flexible KcsA channel annihilates the selectivity of the site S_2, which then becomes favourable for Na^+. The relative free energy, originally unfavourable for Na^+ by 5.3 kcal mol^{-1}, becomes favourable by -2.9 kcal mol^{-1} with a net loss of 8.2 kcal mol^{-1} in selectivity when the repulsive interaction between the backbone carbonyl is turned off (Table 1). *Ab initio* computations on model systems indicate that non-additive electronic polarization (neglected in the present pair-wise all-atom force field)[28] would make the free-energy contribution arising from carbonyl–carbonyl repulsion even more unfavourable. Very strong positional energy restraints (30 kcal mol^{-1} Å^{-2}) must be applied to the KcsA atoms to maintain a selectivity of about 5 to 6 kcal mol^{-1} in the absence of the carbonyl–carbonyl repulsion, essentially freezing the channel. The magnitude of the free-energy change in liquid NMA (10.5 kcal mol^{-1}) is very similar to that found in the fully flexible KcsA channel, suggesting that the coordination of the ions in the selectivity filter of KcsA is indeed very dynamical and 'liquid-like'. Consistent with this view, the width of the main peak in the radial distribution between the cation and the surrounding oxygen ligands shown in Fig. 2 is similar for KcsA and liquid NMA (of the order of 1.0 Å).

To further assess the importance of protein rigidity relative to the local interactions, additional FEP calculations were performed, keeping all channel atoms fixed except those forming the selectivity filter (that is, the backbone atom of residues Thr 74 to Asp 78). In particular, the aromatic side chains suggested to play an essential role in the selectivity (that is, Tyr 78, Trp 67, Trp 68)[5] were kept frozen at their X-ray structure positions. Removing carbonyl repulsion in the selectivity filter results in a loss of almost 6 kcal mol^{-1} of selectivity for K^+ over Na^+ (Table 1), despite the frozen protein surrounding the selectivity filter. Although most conserved residues are essential for the overall stability of the three-dimensional fold (within ~1 Å), the FEP calculations show that the architectural sub-ångstrom rigidity of the protein conferred by the residues surrounding the selectivity filter is not a key factor in making the channel selective for K^+ over Na^+.

Despite its large impact on the relative free energy of solvation of cations in the pore, the carbonyl–carbonyl ligand repulsion has a moderate influence on pore structure. On average, the repulsion between the eight carbonyl groups renders the system 14 kcal mol^{-1} less stable when Na^+ occupies the S_2 site than when K^+ is present. This difference is much smaller than the large interaction energy between the cation and its surroundings (roughly -150 and -170 kcal mol^{-1} for K^+ and Na^+, respectively). The local coordination structure is thus controlled by the strong ion–carbonyl interactions, with K^+ as well as Na^+ being well-coordinated in the flexible and fluctuating pore; see the radial distribution function between the central cation (K^+ or Na^+) and its coordinating oxygens (Fig. 2). In fact, the average structure is not strongly affected when removing the electrostatic repulsion between the carbonyl groups; for example, the coordination numbers with and without repulsion are quite similar (Fig. 2). The carbonyl–carbonyl repulsion thus has little effect on the pore radius, but instead influences ion-binding energetics. This is in accord with behaviour generally seen in flexible systems undergoing thermal fluctuations (for example, a liquid), where the harshest and strongest interactions dictate the average structure while weaker interactions modulate thermodynamics (for example, the core repulsion and London dispersion in a van der Waals liquid)[29].

The ion selectivity of valinomycin is higher than that of KcsA and liquid NMA, although the trends are qualitatively similar (Table 1). As indicated by the narrow width of the radial distribution function (Fig. 2), this cyclic ionophore is more rigid and less able to adapt to coordinate Na^+ than KcsA or liquid NMA as a result of its high covalent connectivity (only three chemical bonds separate each carbonyl group from its neighbours). K^+ is coordinated by six carbonyl oxygen atoms, whereas Na^+ is coordinated by only four carbonyl oxygens (Fig. 2), which increases ion selectivity. In contrast, the selectivity filter of KcsA and liquid NMA are more flexible

Table 1 **Importance of carbonyl–carbonyl repulsion on free energy**

System	ΔΔ*G* with all interactions (kcal mol^{-1})	ΔΔ*G* with no repulsion (kcal mol^{-1})	Loss in ion selectivity (kcal mol^{-1})
Fully flexible KcsA	5.3	−2.9	8.2
Fully frozen KcsA	9.7	9.7	0.0
Restrained KcsA	8.6	5.9	2.7
Partly frozen KcsA	6.7	0.9	5.8
Liquid NMA	1.6	−8.9	10.5
Valinomycin	8.8	3.9	4.9

All calculations with KcsA concern exclusively the S_2 binding site and are based on the X-ray structure PDB id 1K4C. Fully flexible KcsA, all-atom MD/FEP with fully flexible KcsA embedded in DPPC membrane. Fully frozen KcsA, all-atom MD/FEP with KcsA embedded in DPPC membrane with all channel atoms frozen in the X-ray position. Restrained KcsA, all-atom MD/FEP with KcsA embedded in DPPC membrane with all non-hydrogen channel atoms submitted to a harmonic restraint of 30 kcal mol^{-1} Å^{-2} relative to the X-ray position, yielding RMS fluctuations of 0.11 Å for the backbone of the selectivity filter. Partly frozen KcsA, all-atom MD/FEP with KcsA embedded in DPPC membrane allowing motions only for the backbone atoms of the selectivity filter (residues Thr 74 to Asp 78), all other channel atoms are frozen in the X-ray position. Liquid NMA, relative solvation free energy between liquid water and liquid NMA. Valinomycin, relative free energy of ions bound to valinomycin solvated in ethanol.

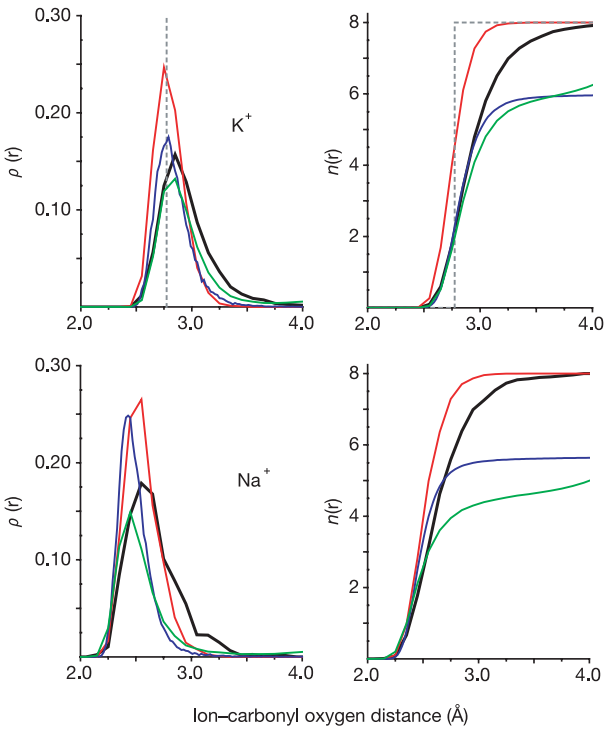

Figure 2 Ion–carbonyl oxygen pair correlation function $\rho(r)$ and coordination number $n(r)$ in different environments. The results for the S_2 binding site of the KcsA selectivity filter with all interactions (solid black line) and without the carbonyl–carbonyl repulsion (solid red line) are shown for K^+ (top) and Na^+ (bottom). For comparison, the corresponding quantities are shown for the X-ray structure (dotted black line), liquid NMA (solid blue line) and in valinomycin (solid green line). The shift in the position of the maximum in the radial distribution for both ions in the selectivity filter of KcsA when carbonyl repulsion is excluded is less than 0.1 Å, much smaller than the width of the main peak (~1.0 Å). In comparison, the shift in the peak position is about 0.32 Å between K^+ and Na^+ when all interactions are included.

than valinomycin. In liquid NMA, K^+ and Na^+ are coordinated by six carbonyl oxygens whereas they are coordinated by six to eight oxygens in the binding site S_2 of KcsA. The coordination structure is liquid-like in both cases, but selectivity is more pronounced for the site S_2 of KcsA than for liquid NMA (see Supplementary Information). Further analysis with a simple model suggests that one mechanism for increasing selectivity in a flexible structure is to increase the number of coordinating ligands surrounding the cation (see below).

Although this is not the underlying mechanism of selectivity, the pore is nonetheless structurally well-adapted to coordinate K^+ with minimal structural strain. For example, the peak in the K^+–oxygen radial distribution function corresponds to the X-ray structure (Fig. 2). The adaptation of the protein surrounding the selectivity filter is perhaps best illustrated by considering the results of *ab initio* geometry optimization of K^+ in the central binding site S_2. Representing the four subunits forming the binding site as glycine dipeptides, the optimized *ab initio* geometry is seen to depart by 0.28 Å r.m.s. from the high-resolution X-ray structure of KscA. Such a relatively small deviation (in the absence of the rest of the protein) suggests that the channel has evolved to optimize the location and structure of the ligands coordinating K^+. But selectivity would be highly sensitive to the sub-ångstrom precision of the selectivity filter if such structural adaptation translated into structural rigidity: additional *ab initio* calculations show that deviation of the four subunits from the optimized configuration by a mere 0.15 Å would be sufficient to abolish the preference for K^+ if the structure were static. Remarkably, thermal fluctuations have the ability to protect the selectivity of the pore for K^+ against such minor structural changes. To illustrate this unexpected feature of a dynamical fluctuating pore, a reduced model limited to the cation-binding site S_2 was considered. This simple model, comprising only 37 atoms, is depicted in Fig. 3a (see legend for details). Similar FEP calculations were repeated, imposing restraints on the atoms of the model to control the magnitude of atom fluctuations in the system. The dependence of $\Delta\Delta G$ on the magnitude of the allowed r.m.s. atomic fluctuations is plotted in Fig. 3b. As expected, the free energies of selectivity are quite similar with and without carbonyl repulsions if atomic fluctuations smaller than 0.1 Å are permitted. But when the repulsion between the carbonyls is removed, the site becomes progressively more selective for Na^+ as the flexibility of the model increases. To ascertain the importance of the geometry of the binding site, FEP calculations were repeated using a model of S_2 optimized for coordinating Na^+ as a reference structure. As shown in Fig. 3b, this binding site is very favourable for Na^+ as long as the system is kept rigid and only atomic fluctuations smaller than 0.3 Å are allowed. But this enforced binding preference is destroyed as thermal fluctuations become larger, with selectivity for K^+ over Na^+ restored as thermal fluctuations of ~0.7 Å are allowed, effectively 'rescuing' the intrinsic binding propensity of the site. Selectivity is thus clearly a robust feature by virtue of the flexible and fluctuating

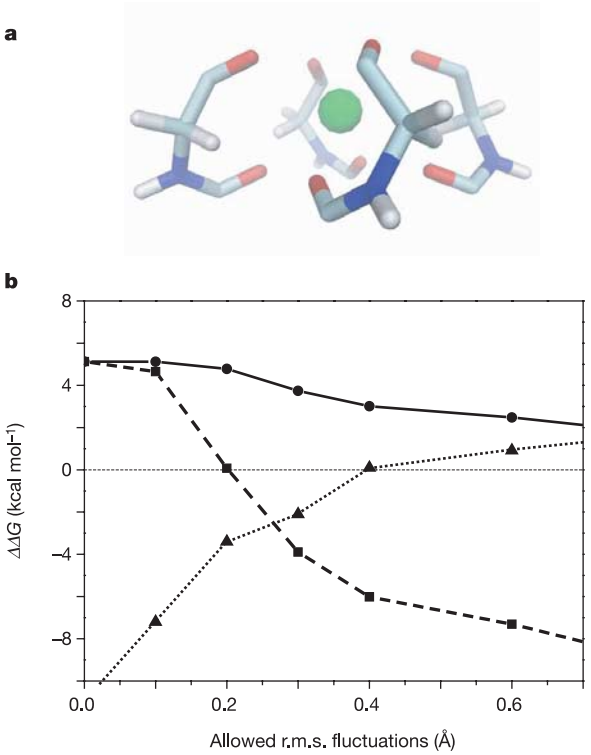

Figure 3 Selectivity of a model of the KcsA binding site S_2 as a function of flexibility. **a**, The structure of the model used to mimic the site S_2 is shown. **b**, The results of the FEP calculations using the X-ray structure of KcsA[7] as a reference with all interactions (solid line with circles) and excluding the carbonyl–carbonyl repulsion (dashed line with squares) are shown. The results of the FEP calculations using a reference structure optimized to best-coordinate a smaller cation such as Na^+ ion in the binding site (obtained via energy minimization in vacuum) are also shown (dotted line with triangles). In all cases, the maximum r.m.s. fluctuations were controlled using a flat-bottomed steep harmonic potential imposed on all the non-hydrogen protein atoms of the model.

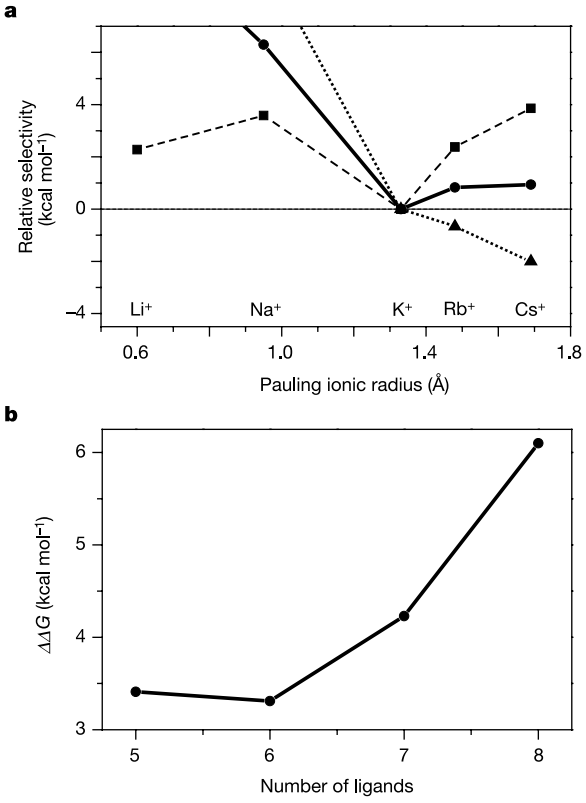

Figure 4 Intrinsic selectivity of a simple model of freely fluctuating carbonyl-like dipoles. **a**, The variations of $\Delta\Delta G$ as a function of ionic radius are shown. The calculations are based on the FEP computations done on a simple model of one cation surrounded by eight carbonyl-like dipoles (comprising two atoms) with the oxygen atoms allowed to move freely within a sphere of radius 3.5 Å. Different cases are illustrated: cation surrounded by eight dipoles of 3.0 debye (solid black line with circles); eight dipoles of 4.2 debye (dashed line with squares) and eight dipoles of 1.8 debye (dotted line with triangles). The results of the FEP calculations for the five cations are plotted using standard ionic radii[14] (the $\Delta\Delta G$ values for the different cases were shifted to bring K^+ to zero). **b**, The dependence of $\Delta\Delta$G on the number of surrounding carbonyl-like dipoles is illustrated. The selectivity is strongly influenced by the number of carbonyl–carbonyl repulsive pairs (that is, $n(n-1)/2$ for n carbonyl groups).

nature of the system, with carbonyl–carbonyl repulsion ensuring the system's selectivity for K^+ binding.

The present analysis shows that ionic selectivity in K^+ channels is primarily determined by the intrinsic physical properties of the ligands coordinating the cation in the binding site, rather than by the precise sub-ångstrom geometry of the carbonyl oxygens lining a rigid pore. While this perspective contrasts sharply with structure-based views of ionic selectivity in K^+ channels[1,5,7], it shares some of the underlying principles of treatments that identify the strength of the electric field arising from the ligands coordinating the cation in a binding site as a key factor in determining selectivity[4]. In this context, we assess the magnitude of the ligand dipoles required to maintain a robust ionic selectivity in a flexible system undergoing thermal fluctuations. We consider a simple model with eight carbonyl-like (C = O) dipoles surrounding a central cation fluctuating freely inside a sphere of 3.5 Å radius. The FEP calculations depicted in Fig. 4 (see legend for details) reveal that such a simple system is naturally selective for K^+ if the ligand dipoles have a magnitude of about 3 debye, a value that is very close to the dipole moment of the protein backbone carbonyl group[28]. This result further demonstrates that significant selectivity for K^+ over Na^+ is possible without any need for architectural rigidity that would prevent the coordinating ligands from collapsing onto a smaller cation.

The main findings from the simple model are consistent with the existence of the conserved TTVGYG motif, which is structurally needed to fold the polypeptide chain into the ion-conducting conformation with the main-chain carbonyl oxygens oriented towards a central pore axis[5]. The selectivity displayed by the simple model is sensitive to the number of coordinating groups; significant selectivity for K^+ over Na^+ is obtained only when eight freely fluctuating carbonyl-like dipoles are present (Fig. 4b). This explains the origin of the low K^+ selectivity in liquid NMA with six nearest neighbours in the first solvation shell (Fig. 2). It also suggests that the three-dimensional fold of the selectivity filter (Fig. 1) might serve to enhance the local 'concentration' of fluctuating carbonyl groups within a small region. The simple model with freely fluctuating carbonyl dipoles leaves out any factors related to protein geometry and rigidity, yet displays qualitative trends in good accord with experimental observations: the selectivity for K^+ over Na^+ is of the order of 5–6 kcal mol^{-1}, whereas the selectivity over Rb^+ and Cs^+ is somewhat smaller[9,10]. The flexible binding site remains optimal for K^+ as long as the coordinating ligands have a dipole roughly between 2.5 and 4.5 debye, that is, are carbonyl-like. Increasing the magnitude of the dipoles beyond 4.5 debye favours smaller cations, whereas decreasing the dipoles has the opposite effect (Fig. 4a). However, decreasing the magnitude of only four out of eight carbonyl dipoles does not alter the selectivity significantly, in accord with experiments introducing a backbone ester carbonyl mutation in the selectivity filter[30]. These observations are consistent with the classical concept of 'field strength' developed by Eisenman[4], although the present analysis incorporates also the influence of thermal atomic fluctuations and ligand–ligand repulsion.

A sharp departure from eight identical carbonyl-like fluctuating ligands is required to make the site favourable for Na^+ over K^+; for example, it becomes selective for Na^+ when the magnitude of the dipoles is ~7 debye. One possible way of achieving Na^+ selectivity (although there are others) would be the introduction of charged residues forming a salt bridge directly into the pore. It is intriguing that the amino acids identified to be essential for the selectivity of Na-channels include the highly conserved DEKA locus from four different protein domains[10,31]. Selectivity for K^+ or for Na^+ clearly requires different chemical functionalities to coordinate the cation favourably, in accord with the observation that no biological channels selective to Na^+ appear to have evolved by refining the geometry of a KcsA-like pore lined by backbone carbonyl groups[10]. □

Methods

Models

The atomic system and simulation methodology have been described elsewhere[19]. Briefly, the total number of atoms in protein simulations is slightly above 40,000 (KcsA, 112 dipalmitoyl phosphatidylcholine, 6,778 water molecules, three K^+ ions in the pore, six K^+ and 21 Cl^- ions in the bulk solutions). The high-resolution structure of the channel was used[7]. The X-ray coordinates were relaxed by less than 0.12 Å to remove any strain in the reference structure. The simple model system for the S_2 binding site occupied by a K^+ (37 atoms with one cation) was taken directly from this structure (Fig. 3a). The corresponding model system for the S_2 binding site occupied by a Na^+ was refined by energy minization in vacuum to generate an optimal coordination for this cation; the resulting structure retained the overall four-fold symmetry but was slightly collapsed onto the smaller cation, deviating from the original structure with K^+ by about 0.51 Å. Two different starting configurations of KcsA embedded in a solvated lipid membrane ('S_0:S_2:S_4' and 'S_1:S_3:cavity') were prepared using the previously published protocols[19]. The FEP computations on the binding sites of KcsA were carried using those configurations, alchemically transforming one cation at a time. FEP simulations of ion solvation in liquid NMA were carried out using a cubic box of 150 NMA molecules and one ion. FEP simulations of ion selectivity in valinomycin were carried out using a cubic box of 225 ethanol molecules. See Supplementary Information for more detail about the NMA and valinomycin systems.

Computational procedure

All MD simulations and FEP computations were carried out using a modified version of the program CHARMM[32]. The total length of simulation preceding the FEP computations was over 1.8 ns. The resulting structure was used to perform the FEP calculations in each binding sites (Fig. 1). The variation in $\Delta\Delta G$ along the pore is associated with the hydration of the cation in the different binding sites (Fig. 1); similar results[19] were obtained using the X-ray structure at lower resolution[5]. The binding sites S_1 and S_3 near the ends of the selectivity filter are less selective (cations in those sites are not completely dehydrated, but maintain some contacts with one or two water molecules) whereas a cation in S_2 is completely dehydrated and coordinated by eight backbone carbonyl oxygens (from Gly 77 and Val 76). To remove the carbonyl–carbonyl repulsion, the Coulomb interactions between those atoms were simply skipped from the main loop in the total energy and forces calculation (this procedure differs from a direct scaling of the partial charges of the carbonyl to zero, because all the electrostatic interactions of the carbonyl with the ions, water molecules and with the remainder of the system remain unaffected). The selectivity filter simulated with and without carbonyl repulsion deviate only by 0.5 Å from one another (the average r.m.s. relative to the X-ray structure is 0.7 Å with repulsion and 0.6 Å without repulsion).

For each of the FEP computation (KcsA, valinomycin, liquid NMA, and the simple models used in Figs 3 and 4), the forward and backward directions free-energy perturbation ($K^+ \leftrightarrow Na^+$) had values of coupling parameter λ varying from 0 to 1 by increments of 0.05 for a total 1.1 ns. All calculations with the frozen or restrained channel structure were carried out according to the same FEP protocol (except that all or some channel atoms are kept fixed at all times) as described previously[19]. The potential function of the ions was parameterized to yield an accurate description of solvation in bulk water and liquid amides. The Lennard–Jones parameters for cations were adjusted to reproduce the experimental free energies of solvation as described previously[19]. Solvation free energies in water were calculated using FEP. For the rest of the atoms, the standard PARAM-22 force field was used[28]. To assess the importance of non-additive forces associated with induced electronic polarization on the FEP computations, *ab initio* computations were performed for a model system of two NMA molecules coordinating one cation (K^+ or Na^+; the results are given in the Supplementary Information).

Received 28 April; accepted 17 August 2004; doi:10.1038/nature02943.

1. Hille, B., Armstrong, C. M. & MacKinnon, R. Ion channels: From idea to reality. *Nature Med.* **5,** 1105–1109 (1999).
2. Zaccai, G. How soft is a protein? A protein dynamics force constant measured by neutron scattering. *Science* **288,** 1604–1609 (2000).
3. Karplus, M. & Petsko, G. A. Molecular dynamics simulations in biology. *Nature* **347,** 631–639 (1990).
4. Eisenman, G. Cation selective electrodes and their mode of operation. *Biophys. J.* **2,** 259–323 (1962).
5. Doyle, D. A. *et al.* The structure of the potassium channel: molecular basis of K^+ conduction and selectivity. *Science* **280,** 69–77 (1998).
6. Morais-Cabral, J. H., Zhou, Y. F. & MacKinnon, R. Energetic optimization of ion conduction rate by the K^+ selectivity filter. *Nature* **414,** 37–42 (2001).
7. Zhou, Y., Morais-Cabral, J. H., Kaufman, A. & MacKinnon, R. Chemistry of ion coordination and hydration revealed by a K^+ channel-Fab complex at 2.0 Å resolution. *Nature* **414,** 43–48 (2001).
8. Eisenman, G. & Horn, R. Ion selectivity revisited: the role of kinetic and equilibrium processes in ion permeation through channels. *J. Membr. Biol.* **76,** 197–225 (1983).
9. Latorre, R. & Miller, C. Conduction and selectivity in potassium channels. *J. Membr. Biol.* **71,** 11–30 (1983).
10. Hille, B. *Ion Channels of Excitable Membranes* 3rd edn (Sinauer, Sunderland, Massachusetts, 2001).
11. Neyton, J. & Miller, C. Discrete Ba^{2+} block as a probe of ion occupancy and pore structure in the high-conductance Ca^{2+}-activated K^+ channel. *J. Gen. Physiol.* **92,** 569–596 (1988).
12. LeMasurier, M., Heginbotham, L. & Miller, C. KscA: it's a potassium channel. *J. Gen. Physiol.* **118,** 303–314 (2001).
13. Nimigean, C. M. & Miller, C. Na^+ block and permeation in K^+ channel of known structure. *J. Gen. Physiol.* **120,** 323–325 (2002).
14. Pauling, L. *Nature of the Chemical Bond and Structure of Molecules and Crystals* 3rd edn (Cornell Univ. Press, Ithaca, 1960).
15. Allen, T. W., Andersen, O. S. & Roux, B. On the importance of atomic fluctuations, protein flexibility

and solvent in ion permeation. *J. Gen. Physiol.* (in the press).
16. Åqvist, J. & Luzhkov, V. Ion permeation mechanism of the potassium channel. *Nature* **404,** 881–884 (2000).
17. Luzhkov, V. B. & Åqvist, J. K^+/Na^+ selectivity of the KcsA potassium channel from microscopic free energy perturbation calculations. *Biochim. Biophys. Acta* **1548,** 194–202 (2001).
18. Allen, T. W., Bliznyuk, A., Rendell, A. P., Kyuucak, S. & Chung, S. H. The potassium channel: Structure, selectivity and diffusion. *J. Chem. Phys.* **112,** 8191–8204 (2000).
19. Bernèche, S. & Roux, B. Energetics of ion conduction through the K^+ channel. *Nature* **414,** 73–77 (2001).
20. Bernèche, S. & Roux, B. A microscopic view of ion conduction through the K^+ channel. *Proc. Natl Acad. Sci. USA* **100,** 8644–8648 (2003).
21. Shrivastava, I. H., Tieleman, D. P., Biggin, P. C. & Sansom, M. S. P. K^+ versus Na^+ ions in a K channel selectivity filter: A simulation study. *Biophys. J.* **83,** 633–645 (2002).
22. Guidoni, L., Torre, V. & Carloni, P. Potassium and sodium binding to the outer mouth of the K^+ channe. *Biochemistry* **38,** 8599–8604 (1999).
23. Loboda, A., Melishchuk, A. & Armstrong, C. Dilated and defunct K channels in the absence of K^+. *Biophys. J.* **80,** 2704–2714 (2001).
24. Zhou, Y. F. & MacKinnon, R. The occupancy of ions in the K^+ selectivity filter: Charge balance and coupling of ion binding to a protein conformational change underlie high conduction rates. *J. Mol. Biol.* **333,** 965–975 (2003).
25. Yamashita, M. M., Wesson, L., Eisenman, G. & Eisenberg, D. Where metal ions bind in proteins. *Proc. Natl Acad. Sci. USA* **87,** 5648–5652 (1990).
26. Åqvist, J., Alvarez, O. & Eisenman, G. Ion-selective properties of a small ionophore in methanol studied by free energy perturbation simulations. *J. Phys. Chem.* **96,** 10019–10025 (1992).
27. Marrone, T. J. & Merz, K. M. Jr. Molecular recognition of K^+ and Na^+ by valinomycin in methanol. *J. Am. Chem. Soc.* **117,** 779–791 (1995).
28. MacKerell, A. D. J. *et al.* All-atom empirical potential for molecular modeling and dynamics studies of proteins. *J. Phys. Chem. B* **102,** 3586–3616 (1998).
29. Weeks, J. D., Chandler, D. & Andersen, H. C. Role of repulsive forces in determining the equilibrium structure of simple liquids. *J. Chem. Phys.* **54,** 5237–5247 (1971).
30. Lu, T. *et al.* Probing ion permeation and gating in a K^+ channel with backbone mutations in the selectivity filter. *Nature Neurosci.* **4,** 239–246 (2001).
31. Heinemann, S. H., Terlau, H., Stuhmer, W., Imoto, K. & Numa, S. Calcium channel characteristics conferred on the sodium channel by single mutations. *Nature* **356,** 441–443 (1992).
32. Brooks, B. R. *et al.* CHARMM: a program for macromolecular energy minimization and dynamics calculations. *J. Comput. Chem.* **4,** 187–217 (1983).

Supplementary Information accompanies the paper on **www.nature.com/nature**.

Acknowledgements Discussions with G. Eisenman, J. Åqvist, O. Andersen, C. Miller and D. Doyle are gratefully acknowledged. This work was funded by the NIH and by the American Epilepsy Society and UCB Pharma Inc. to S.Yu.N. This work was supported by the National Center for Supercomputing Applications (NCSA) at the University of Illinois, Urbana-Champaign, the Pittsburgh Supercomputing Center (PSC), and the Scientific Computing and Visualization (SCV) group at Boston University.

Competing interests statement The authors declare that they have no competing financial interests.

Correspondence and requests for materials should be addressed to B.R. (benoit.roux@med.cornell.edu).

Low marine sulphate and protracted oxygenation of the Proterozoic biosphere

Linda C. Kah[1], Timothy W. Lyons[2] & Tracy D. Frank[3]

[1]*Department of Earth and Planetary Sciences, University of Tennessee, Knoxville, Tennessee 37996, USA*
[2]*Department of Geological Sciences, University of Missouri, Columbia, Missouri 65211, USA*
[3]*Department of Geosciences, University of Nebraska, Lincoln, Nebraska 68588, USA*

Progressive oxygenation of the Earth's early biosphere is thought to have resulted in increased sulphide oxidation during continental weathering, leading to a corresponding increase in marine sulphate concentration[1]. Accurate reconstruction of marine sulphate reservoir size is therefore important for interpreting the oxygenation history of early Earth environments. Few data, however, specifically constrain how sulphate concentrations may have changed during the Proterozoic era (2.5–0.54 Gyr ago). Prior to 2.2 Gyr ago, when oxygen began to accumulate in the Earth's atmosphere[2,3], sulphate concentrations are inferred to have been <1 mM and possibly <200 μM, on the basis of limited isotopic variability preserved in sedimentary sulphides[4] and experimental data showing suppressed isotopic fractionation at extremely low sulphate concentrations[1,5]. By 0.8 Gyr ago, oxygen and thus sulphate levels may have risen significantly[6,7]. Here we report large stratigraphic variations in the sulphur isotope composition of marine carbonate-associated sulphate, and use a rate-dependent model for sulphur isotope change that allows us to track changes in marine sulphate concentrations throughout the Proterozoic. Our calculations indicate sulphate levels between 1.5 and 4.5 mM, or 5–15 per cent of modern values, for more than 1 Gyr after initial oxygenation of the Earth's biosphere. Persistence of low oceanic sulphate demonstrates the protracted nature of Earth's oxygenation. It links biospheric evolution to temporal patterns in the depositional behaviour of marine iron- and sulphur-bearing minerals[4], biological cycling of redox-sensitive elements[6] and availability of trace metals essential to eukaryotic development[8].

To understand Proterozoic biospheric oxygenation better, we have modified an existing model for C isotope variability[9] to estimate marine sulphate reservoir size using rates of S isotope variation. These rates are recorded stratigraphically as variation in the S isotope composition of evaporitic gypsum and carbonate-associated sulphate (CAS). Because CAS is routinely trapped in marine carbonates[10] and, in organic-poor sediments, is isotopically buffered against appreciable diagenetic overprints[11], it can record the $\delta^{34}S$ signal of marine sea water even when gypsum is lacking. Furthermore, CAS is a more direct proxy for marine sea water than sedimentary pyrite, the isotopic composition of which is complicated by local reservoir effects and varying fractionations during bacterial sulphate reduction (BSR)[12].

In our model, the isotopic composition of marine sulphate changes in response to imbalances in isotopic fluxes into and out of a non-steady state system (see Methods). In the modern ocean, sulphate concentrations of 28.4 mM effectively buffer the isotopic system from changing at rates exceeding 0.5‰ per Myr, despite large fractionations associated with the modern bacterial sulphur cycle (Fig. 1). Long-term variation in the isotopic composition of

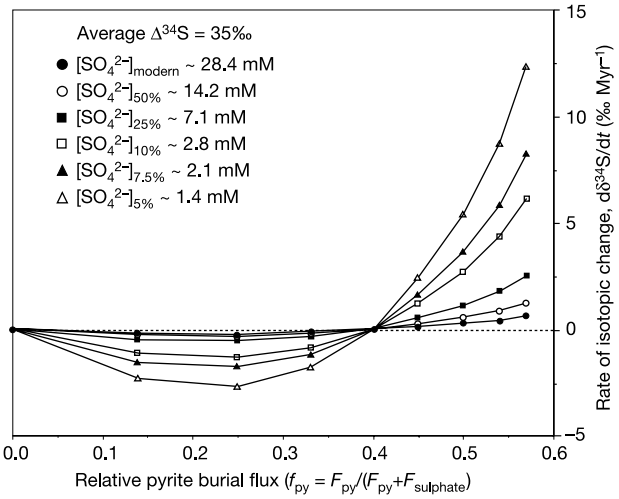

Figure 1 Sensitivity of the marine sulphate system to reservoir size. At average fractionations observed within the modern bacterial sulphur cycle ($\Delta S = 35‰$), modern reservoir sizes effectively buffer the marine system from the large S isotope shifts that characterize Proterozoic stratigraphic sections, even at moderate to high degrees of pyrite burial ($f_{py} = 0.2–0.6$).

Supplementary material.

A) Crystallographic thermal B-factors of the KcsA channel

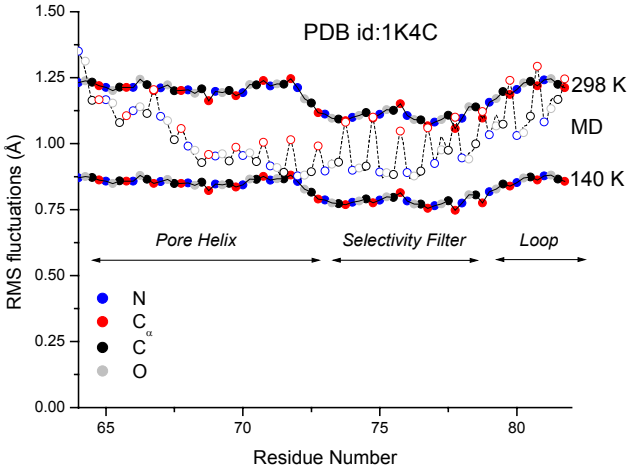

The RMS atomic fluctuations (defined as $<\Delta \boldsymbol{R}^2>^{1/2}$) extracted from the isotropic Debye-Waller crystallographic thermal B-factors of the KcsA channel structure solved at 2.0 Å resolution in complex with a FAB antibody fragment[1] (PDB databank ID 1K4C) are compared with the results from the current molecular dynamics simulation. The B-factors of the backbone atoms of the selectivity filter KcsA are in the range of 15 to 20 $Å^2$. In principle, the B-factors are directly related to the RMS atomic fluctuations with $B=(8\pi^2/3)<\Delta \boldsymbol{R}^2>$.[2,3] However, interpretation of the B-factors requires some care[4] because the crystals were fast-frozen in liquid nitrogen[1] and the diffraction data was obtained under a flow of liquid nitrogen vapor according to a standard protocol (temperature around 120 to 140 K). A lower bound to the RMS fluctuations is obtained directly from the experimental B-factors, based on the assumption that all thermal motions were quenched infinitely rapidly upon fast-freezing in liquid nitrogen. This lower bound yields RMS atomic fluctuations in the range of 0.8 to 0.9 Å (data identified as 140 K in the figure). However, fast-freezing is not instantaneous on molecular timescales.[4,5] The RMS fluctuations at room temperature (298 K) can be estimated based on the assumption that the small sub-angstrom librations of the backbone occurring on the picosecond timescale have sufficient time to anneal to the lower temperature upon freezing (140 K). Because the thermal quadratic fluctuations $<\Delta \boldsymbol{R}^2>$ are linearly proportional to the effective temperature in the harmonic approximation,[3] the RMS fluctuations at 298 K can be estimated by scaling the RMS fluctuations at 140 K by $(298/140)^{1/2}$. This yields RMS atomic fluctuations in the range of 1.1o 1.2 Å (data identified as 298 K in the figure). The results from the current molecular dynamics trajectory, shown as open symbols in the figure, falls between the lower and upper estimates from the crystallographic B-factors. An exact correspondence between MD and the estimates extracted from the B-factors is not expected due to uncertainties in the interpretation of the low temperature B-factors. The RMS thermal fluctuations of the backbone atoms of the selectivity filter of the KcsA channel are roughly on the order of 1 Å, similar to that of most proteins and much larger than the size difference between K+ and Na+ (0.38 Å).

B) *Ab Initio* Calculations

All *ab initio* computations were done using Gaussian-98 program suite.[6] The geometry of the complex with K^+ in the S_2 binding site was optimized at Hartree-Fock (HF) level using the split valence 6-31G* basis set starting from the x-ray structure.[1] The backbone of residues Val76-Gly77 was modeled as a glycine-dipeptide with no sidechains for a total of 37 non-hydrogen atoms requiring 1244 primitive gaussians basis functions.

The non-additivity in carbonyl-carbonyl repulsion was estimated using two N-methyl-acetamide molecules coordinating one cation. The geometry of the complex was initially optimized using density functional theory (DFT) with Becke's three-parameter hybrid method[7] in conjunction with the Lee, Yang, and Parr correlation functional (B3LYP)[8] using the split-valence 6-31++G (2d,2p) basis set. Individual contributions to interaction energies were then evaluated from single point calculations with second-order Moller-Plesset perturbation (MP2) using the split valence 6-31++G (2d,2p) basis set. Decomposition of the *ab initio* energies (Table) indicates that non-additive effects are increasingly unfavorable (repulsive) as the radius of the cation gets smaller. Induced polarization contributes an additional +3.8 kcal/mol and +4.4 kcal/mol to the NMA-NMA repulsion in the case of K^+ and Na^+, respectively. Therefore, it can be anticipated that the unfavorable free energy arising from carbonyl-carbonyl repulsion would be reinforced by non-additive electronic polarization.

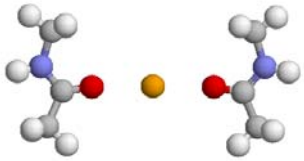

Figure. Complex of one cation with two N-methdyl acetamide (NMA) molecules in the optimized geometry used to estimate the non-additive induced polarization interactions.

Table. Energy Decomposition of non-additive interactions (kcal/mol)

Energy term	K^+	Na^+
ΔE_{123}	-56.97	-76.95
ΔE_1	-25.53	-34.71
ΔE_2	-31.44	-42.24
ΔE_3	2.11	3.16
ΔE_4	5.91	7.55
$\Delta\Delta E_{123}$	3.8	4.39
ΔE_{pair}	-29.33	-39.08

Total ion-ligands interaction energy is $\Delta E_{123} = E[\text{ion},NMA_1,NMA_2]-E[NMA_1,NMA_2]-E[\text{ion}]$; Individual interaction energy between ion and 1-st NMA with accounting repulsion from the second NMA is $\Delta E_1 = E[\text{ion},NMA_1,NMA_2]-E[NMA_1,\text{ion}]-E[\text{ion}]$; interaction energy between ion and individual NMA: $\Delta E_2 = E[\text{ion},NMA_1]-E[\text{ion}]-E[NMA_1]$; Repulsion between 2 NMA in the absence of the ion is $\Delta E_3 = E[NMA_1,NMA_2]-E[NMA_1]-E[NMA_2]$; Total repulsion energy between 2 NMA in presence of the ion is: $\Delta E_4 = \Delta E_1 - \Delta E_2$; Non-additive correction to the electrostatic repulsion is $\Delta\Delta E_{123} = \Delta E_4 - \Delta E_3$; NMA-ion pair interaction energy without non-additive correction is $\Delta E_{pair} = \Delta E_1 - \Delta\Delta E_{123}$

C) Ion selectivity in valinomycin solvated in ethanol

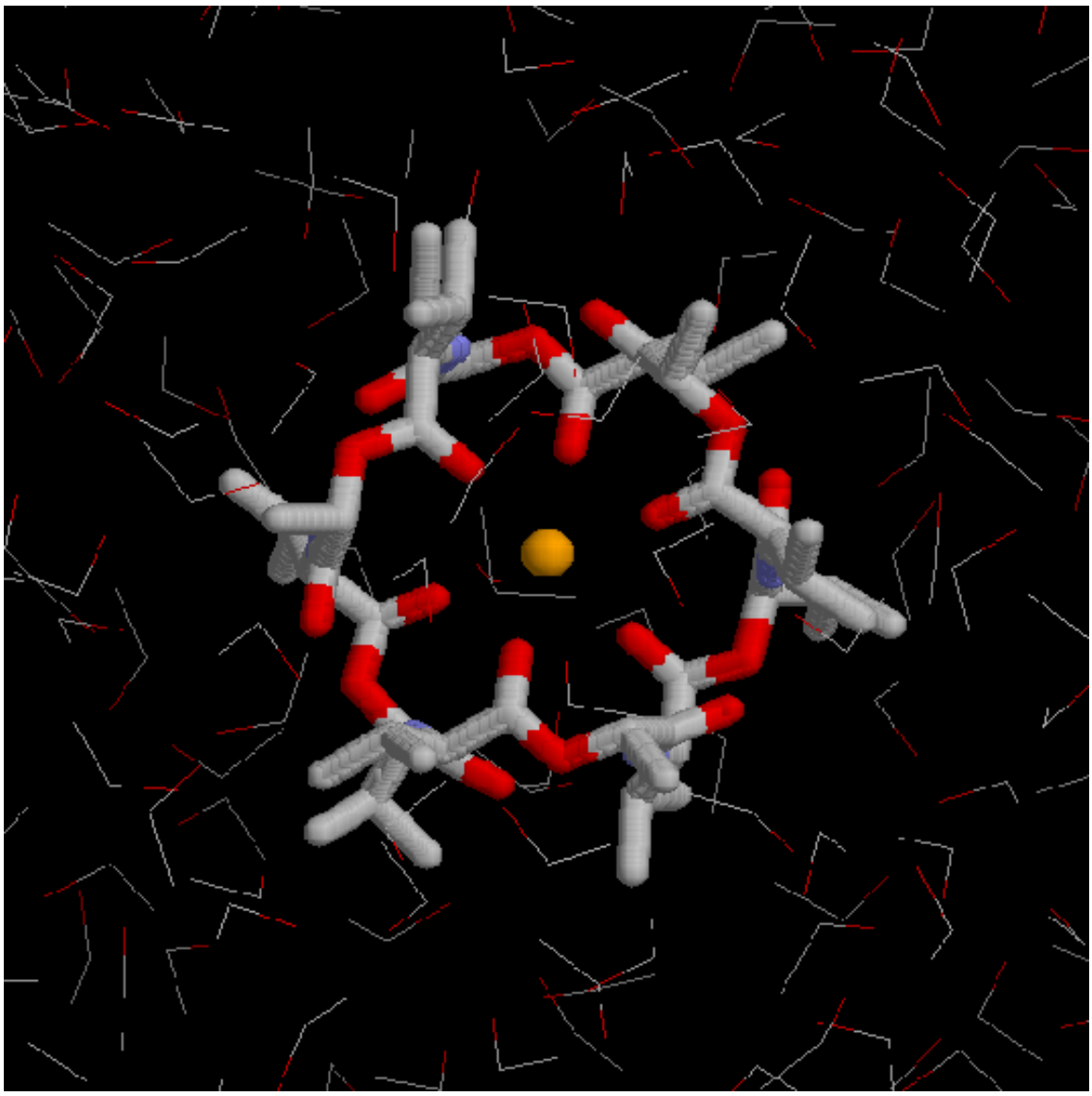

RASMOL respresentation of valinomycin solvated in ethanol. The x-ray structure of a K^+ valinomycin complex[9,10] was used to construct the initial system which was then solvated with 225 ethanol. The cation is coordinated by six carbonyl groups. The system was simulated with cubic periodic boundary conditions. The relative free energy of K^+ and Na^+ was calculated using molecular dynamics free energy simulations:

$$\Delta\Delta G(\mathrm{K}^+ \rightarrow \mathrm{Na}^+) = \left[\left(G_{\text{valinomycin}}(\mathrm{Na}^+) - G_{\text{bulk}}(\mathrm{Na}^+)\right) - \left(G_{\text{valinomycin}}(\mathrm{K}^+) - G_{\text{bulk}}(\mathrm{K}^+)\right)\right]$$

D) Ion solvation in liquid N-methylacetamide

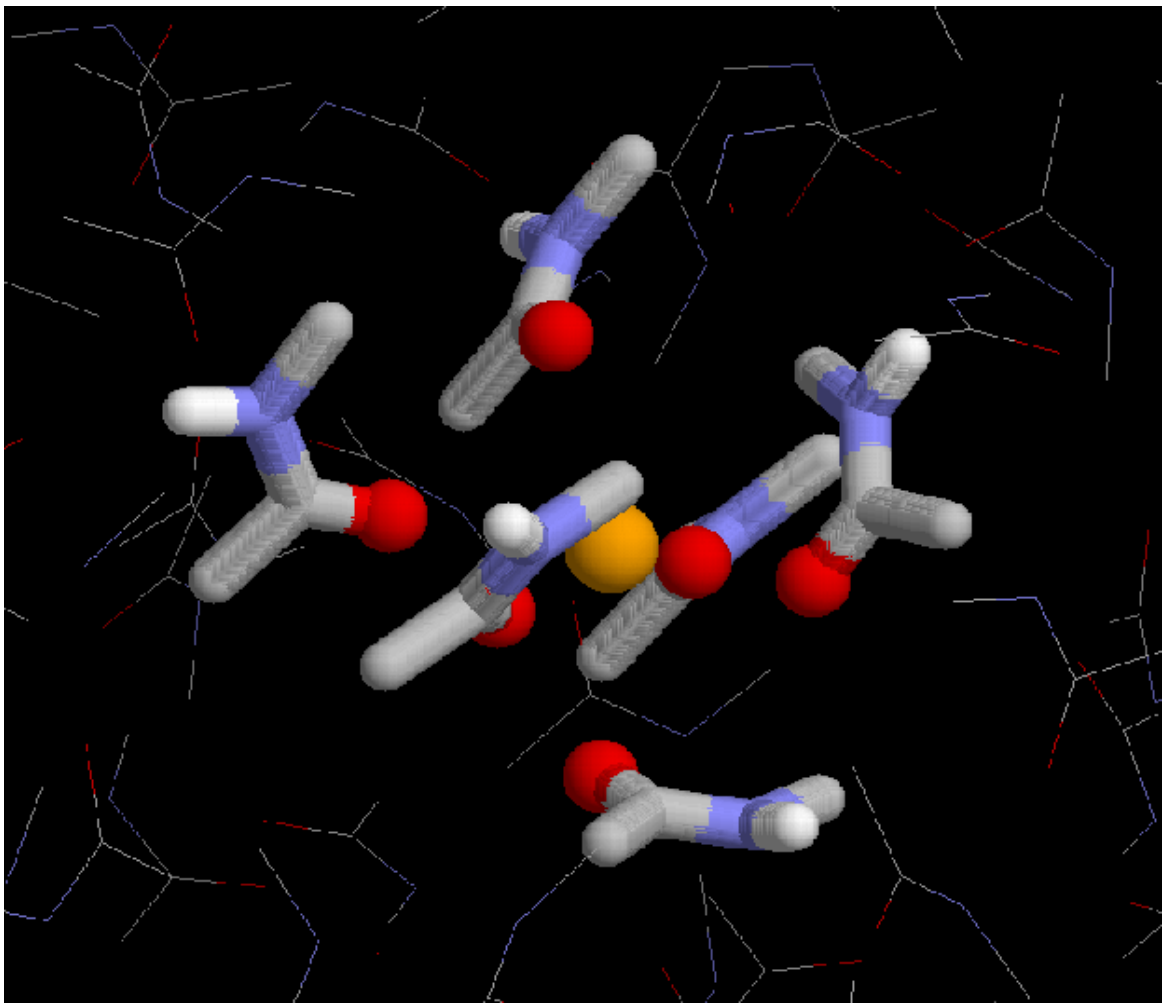

RASMOL representation of ion solvation in liquid N-methyl acetamide. Both K^+ and Na^+ are coordinated by six carbonyl groups in the first solvation shell in a semi-cubic geometry due to packing constraints. The system comprising one cation (K^+ or Na^+) and 150 NMA molecules was simulated with cubic periodic boundary conditions. The relative solvation free energy of K^+ and Na^+ was calculated using molecular dynamics free energy simulations:

$$\Delta\Delta G(\mathrm{K}^+ \rightarrow \mathrm{Na}^+) = \left[\left(G_{\mathrm{NMA}}(\mathrm{Na}^+) - G_{\mathrm{water}}(\mathrm{Na}^+)\right) - \left(G_{\mathrm{NMA}}(\mathrm{K}^+) - G_{\mathrm{water}}(\mathrm{K}^+)\right)\right]$$